crease with other surface geometries. For example, if we take spherically shaped domes and arrange them in the most compact way, the area increase factor is 1.7. Likewise, the development of (100)-type preferred oriented platinum, even under 100% efficiency, would contribute less than 20% real area increase. Therefore, the development of the catalytic activity in the volume of the electroreduced platinum crystallites must play the most important role, as may be concluded from the surface microtopography.

On the basis of these results, the behavior of activated platinum electrodes can be explained by admitting that each pebble-like crystallite can be represented by a sphere of 100 Å average radius. The sphere ensemble is made by piling up the spheres in a volume defined by the geometric electrode area times the average thickness of the electroreduced platinum layer. This thickness can be obtained from the corresponding oxide electroreduction charge; its value for a 100 times activation can be estimated as 5×10^3 Å. This volume structure should be wetted by the electrolyte solution, making the entire surface of each sphere equally accessible to reactants through interconnected inner channels. The number of spheres of 100 Å radius per cm^2 which can be accomodated within the volume of the active electrode is about 10^{12}. Therefore, provided that the entire surface of each sphere is catalytically active, the large activation factor, of the order of 10^2, deduced from the voltammetric charge at 0.2 V/s can be immediately understood.

For an average thickness of about 10^3 Å and diffusion coefficients of the order of 10^{-6} cm^2/s as expected for most ions in aqueous solutions, it is obvious that, even at the rate of 1 V/s, the contribution of diffusional relaxation should become negligible. Hence, under usual voltammetric conditions, this type of platinum electrodes, in contrast to conventional platinized platinum (Figure 1a), should offer practically no anomalous voltammetric response (Figure 1b).

The proposed simple model explains the important fact that the electrocatalytic activation remains practically the same for electrochemical processes occurring in different potential ranges with reactants and intermediates of different sizes, as is the case for hydrogen and oxygen adatom electroadsorption/electrodesorption,[3] adsorbed ethylene electroxidation,[17] and reduced carbon dioxide electroxidation.[18]

Experimental Section

Preparation of the Platinum Electrodes. The preparation of the activated platinum electrode surfaces was made by following the technique already described in the literature.[3] It consisted of a repetitive square wave potential signal (RSWPS) at 2.5 kHz between 0 and 2.3 V applied for a certain time to polycrystalline (pc) platinum electrodes (geometric area ranging from 0.1 to 2 cm^2). The electrodes from Specpure quality Johnson Matthey Chemical Ltd. and Engelhard 99.99% purity were immersed in either 1 M $HClO_4$ or 0.5 M H_2SO_4, at 25 °C. During the RSWPS treatment a relatively thick hydrous platinum oxide layer was formed, whose thickness depended on the duration of RSWPS. Immediately afterwards the hydrous oxide multilayer was electroreduced at 0.01 V/s, yielding the new platinum surface.

Evaluation of Platinum Electrode Roughness. The initial true electrode area was determined through the hydrogen adatom monolayer charge resulting from conventional voltammograms run with triangular potential sweeps at 0.2 V/s between 0.01 and 1.40 V in 0.5 M H_2SO_4 at 25 °C. The average hydrogen adatom monolayer charge was taken as 210 $\mu C/cm^2$.[9-12] The relative increase in the electrode real surface area was evaluated as the ratio between the hydrogen electroadsorption monolayer charge before and after the RSWPS treatment.

STM Measurements. STM data were taken at a tunneling voltage of -10 mV (tip negative) and a tunneling current of 5 nA. A typical scanning frequency was 0.1 Hz. Vertical sensitivity was in the subnanometer range whereas lateral sensitivity was kept in the nanometer range.

Acknowledgment. We acknowledge discussions with J. M. Soler and J. J. Saenz. We also appreciate the very useful help with the electronic equipment from J. Pedrosa.

Registry No. Pt, 7440-06-4; $HClO_4$, 7601-90-3; H_2SO_4, 7664-93-9; H_2, 1333-74-0.

(17) Piovano, E. M.; Chialvo, A. C.; Triaca, W. E.; Arvia, A. J. *J. Appl. Electrochem.*, in press.
(18) Marcos, M. L.; Velasco, J. G.; Vara, J. M.; Arvia, A. J. in preparation.

Bonding Capabilities of Nickel Cluster Ions: Synthetic Chemistry in a Molecular Beam

Pierre Fayet,*† Michael J. McGlinchey,*‡ and Ludger H. Wöste*†

Contribution from the Institut de Physique Expérimentale, Ecole Polytechnique Fédérale de Lausanne, CH-1015 Lausanne, Switzerland, and Department of Chemistry, McMaster University, Hamilton, Ontario, Canada L8S4M1. *Received August 6, 1986*

Abstract: Nickel cluster ions, size-selected by quadrupole mass spectrometry, were treated with carbon monoxide to yield in the gas phase nickel–carbonyl complexes of the type $Ni_n(CO))_k^+$ and $Ni_nC(CO)_l^+$ where n ranges from 1 through 13 and k and l vary as a function of the cluster size n. The stoichiometry of these clusters correlates extremely well with the electron-counting rules proposed by Lauher.

I. Introduction

Over the past 15 years, detailed spectroscopic investigations of matrix isolated atoms and small clusters have provided much insight into catalytic processes occurring on metal surfaces.[1] Nevertheless, it is still extremely difficult to build up a concentration of a single chemical species although some progress has been made by cryophotoclustering techniques.[2] There are obvious attractions to working in the gas phase since one can avoid the complications arising from solvents or from matrix effects.[3]

Molecular beam expansion combined with mass spectrometry is a well-established technique to investigate optical and chemical properties of metal clusters in the gas phase. Experiments,

† Institut de Physique Expérimentale.
‡ McMaster University.

(1) (a) Moskovits, M.; Ozin, G. A. In *Cryochemistry*; Wiley-Interscience: New York, 1976. (b) Burdett, J. K. *Coord. Chem. Rev.* **1978**, *27*, 1. (c) Ozin, G. A. *Ibid.* **1979**, *28*, 117.
(2) Power, W. J.; Ozin, G. A. *Adv. Inorg. Chem. Radiochem.* **1980**, *23*, 79.
(3) (a) Geusic, M. E.; Morse, M. D.; Smalley, R. E. *J. Chem. Phys.* **1986**, *82*, 590. (b) Trevor, D. J.; Whetten, R. L.; Cox, D. M.; Kaldor, A. *J. Am. Chem. Soc.* **1985**, *107*, 518. (c) Richtmeier, S. C.; Parks, E. K.; Liu, K.; Pobo, L. G.; Riley, S. J. *J. Chem. Phys.* **1985**, *82*, 3659.

0002-7863/87/1509-1733$01.50/0

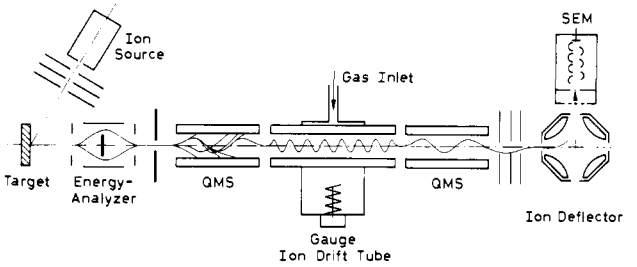

Figure 1. Experimental setup.

however, are strongly handicapped by fragmentation phenomena, which commonly occur during reactive collisions, electronic transitions, neutralization or ionization processes. Therefore, parent molecules and fragments can no longer be easily distinguished.

For this reason we developed an apparatus that allowed us to perform the above-mentioned experiments with naked metal clusters of a specific size and charge. As the cluster source we chose a sputtering arrangement.[4] This allowed us to generate positively and negatively charged clusters as well as neutrals from nearly all materials. The emerging cluster ions were energy-filtered, mass-separated, and then introduced into an ion drift tube where they were kept at low kinetic energy in a radiofrequency confinement. The confined ions were then allowed to interact with carbon monoxide. All collision-induced fragmentations or chemical reactions of the confined cluster ions were then analyzed with another mass spectrometer at the exit of the ion drift tube. The results showed very distinctive properties of individual cluster sizes with respect to stability, structure, and chemical reactivity.

II. Experimental Section

For generating the primary ion beam we used a modified cold reflex discharge ion source (CORDIS),[5] which was developed by R. Keller for use in the heavy ion accelerator at GSI Darmstadt. The ion source is placed inside a differentially pumped vacuum chamber at a distance of 50 cm from the target, with an angle of incidence of 50°. Operating at an ion energy of 20 keV and a primary beam diameter of 10 mm, typical ion currents of 2 mA were measured. The target is mounted on a manipulator device for rapid exchange and optimum positioning. It is temperature controlled and can be kept at any desired bias voltage. A metal cylinder around the target reduces the contamination of the vacuum chamber with sputtering deposits. The system is pumped with a 500 l/s turbomolecular pump.

The kinetic energy distribution of sputtered particles is typically between 0 and 10 eV. A cylindrical retarding field energy analyzer cuts out of this range an energy band of ±2 eV. In addition to that, it blocks all fast primary ions and sputtered neutrals. The energy filter is directly mounted at the entrance of the quadrupole mass filter at a distance of about 4 cm from the target. We used a commercial quadrupole rod-system of 9.5 mm pole diameter and a length of 20 cm (Extranuclear Model 4-162-8), which under normal operating conditions reaches a maximum mass value of 1700.

The monodispersed cluster beam is directly guided from the quadrupole mass filter into the drift tube, which is 60 cm long and has a sectional view identical with that of the mass filter. The drift tube is operated with the same rf as the mass filter at a controlled phase shift. Since, however, no DC voltage is applied, there is no mass discrimination, and all ions, photofragments, and reaction products are kept in confinement. The relative electric potential of the rod system allows the slowing down of the confined ions to almost thermal velocities, which corresponds to residence times up to 10 ms. The drift tube is surrounded by a scatter chamber of 10-cm length where reactant gas is introduced. The complete drift tube assembly is placed inside another differentially pumped ultrahigh vacuum chamber, pumped by a 500 l/s turbomolecular pump. The pressure inside the reaction chamber is measured with an ionization gauge. The background pressure under normal operation conditions is $<10^{-8}$ mbar, which is sufficient to prevent undesired background collisions. It can be operated, however, at pressures up to 10^{-2} mbar, when the reactant gas is introduced (see Figure 1).

At the exit of the drift tube the confined ion beam enters another quadrupole mass filter (Extranuclear Model 4-162-8). It is operated at the same frequency as the first mass filter and the drift tube at a controlled phase shift, and it is placed inside a differentially pumped ultravacuum chamber, pumped by a 500 l/s turbomolecular pump. The same chamber also contains a 21-stage Cu–Be secondary electron multiplier for detecting the ions. It is mounted on an electrostatic ion deflector, in order to allow a laser beam to enter the triple quadrupole system for performing laser-induced photofragmentation experiments.[6]

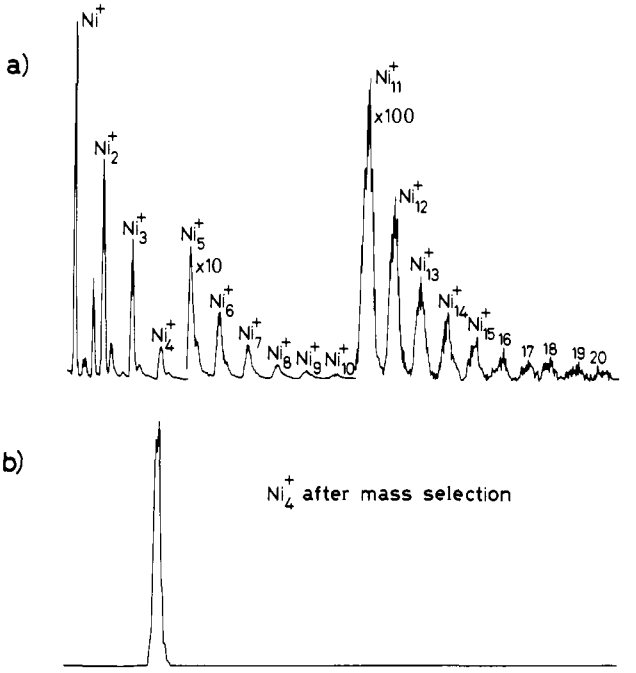

Figure 2. (a) Mass spectrum of positively charged sputtered nickel clusters. Note the sensitivity change at Ni_5^+ and Ni_{11}^+. (b) Mass spectrum of the monodispersed cluster beam, recorded by setting the first QMS in front of the ion drift tube on the mass of Ni_4^+, while the second spectrometer behind the drift tube was scanned.

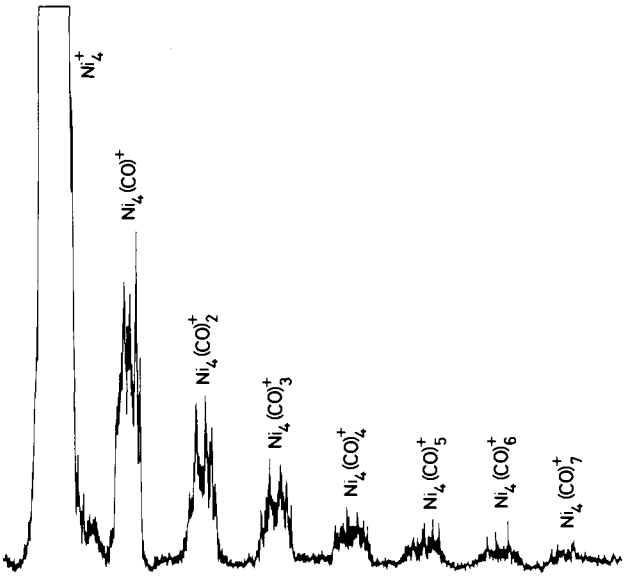

Figure 3. Reactive clustering of CO ligands to a Ni_4^+ cluster by introduction of carbon monoxide into the drift tube.

III. Results

When a nickel target was used, the ions Ni_n^+, where n is 1–20, were produced in monotonically decreasing amounts (see Figure 2a). Upon mass separation, any desired nickel cluster can be selected, and Figure 2b shows the mass spectrum of the cleanly separated tetranickel cation, Ni_4^+. Treatment of this beam of tetranuclear clusters with a low pressure of carbon monoxide and

(4) Devienne, F. M.; Roustan, J. C. *Org. Mass. Spectr.* **1982**, *17*, 173.
(5) Keller, R. *Symp. Acc. Asp. Heavy Ion Fusion*, **1983**.
(6) Fayet, P.; Wöste, L. *Surf. Sci.* **1985**, *156*, 134.

Table I. Maximum Number of CO Ligands as a Function of Cluster Size Following One of the Three Reaction Channels

$$Ni_n^+ + CO \rightarrow \begin{cases} Ni_nC(CO)_l^+ \\ Ni_{(n-1)}(CO)_m^+ \end{cases}$$

cluster	Ni_2^+	Ni_3^+	Ni_4^+	Ni_5^+	Ni_6^+	Ni_7^+	Ni_8^+	Ni_9^+	Ni_{10}^+	Ni_{11}^+	Ni_{12}^+	Ni_{13}^+
k	9	8	10	12	13	15	16	17	18	19	20	22
l	5	7	7	9	11	13	14	12	16	*a*	20	20
m	8	9	11	13	11	14	17	18	19	20	21	22

[a] Not observed.

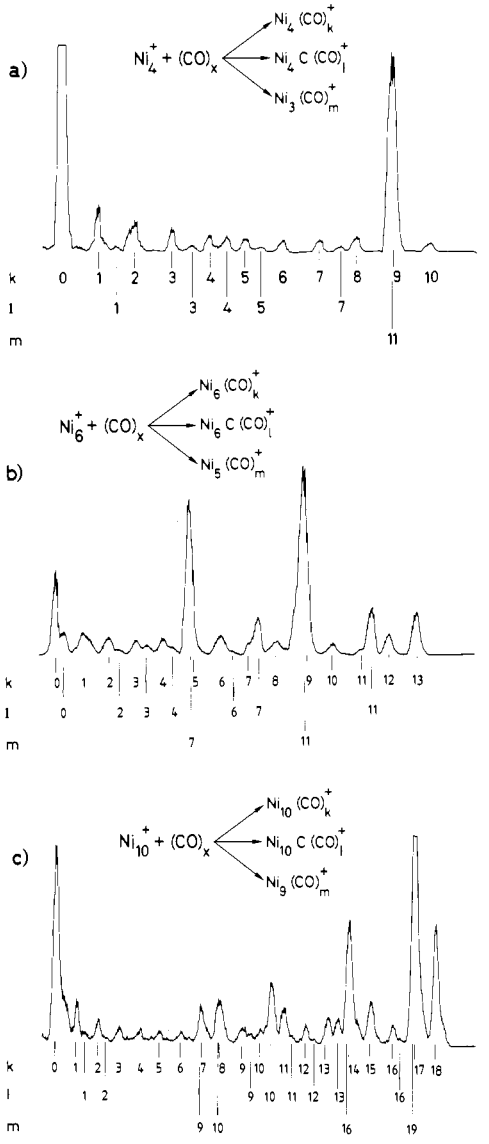

Figure 4. Products of the reaction of carbon monoxide with (a) Ni_4^+, (b) Ni_6^+, and nc) Ni_{10}^+ at a CO pressure of approximately $3 \cdot 10^{-3}$ mbar.

subsequent mass spectrometric analysis of the products reveals the formation of a series of $Ni_4(CO)_k^+$ cluster ions (see Figure 3). The pressure of CO was then gradually increased to the point at which the product spectrum did not change, i.e., when saturation of the cluster with carbon monoxide ligands has occurred (pressure of CO: $2.4\ 10^{-3}$ mbar); this situation is depicted in Figure 4a, and it is apparent that the highest molecular weight ion has the formula $Ni_4(CO)_{10}^+$. However, we see also the development of two more series of cluster ions, viz., tetranickel carbido carbonyls $Ni_4C(CO)_l^+$ and also the trinickel carbonyl clusters $Ni_3(CO)_m^+$ derived via fragmentation processes.

When the mass of the selected cluster was increased to Ni_6^+, and the beam was treated with carbon monoxide as before, the maximum size nickel cluster obtained corresponded to $Ni_6(CO)_{13}^+$, as shown in Figure 4b. The result for Ni_{10}^+ is shown in Figure 4c, where a maximum particle size of $Ni_{10}(CO)_{18}^+$ was observed. The results, which were obtained for all cluster sizes from Ni_2^+ to Ni_{13}^+, are collected in Table I.

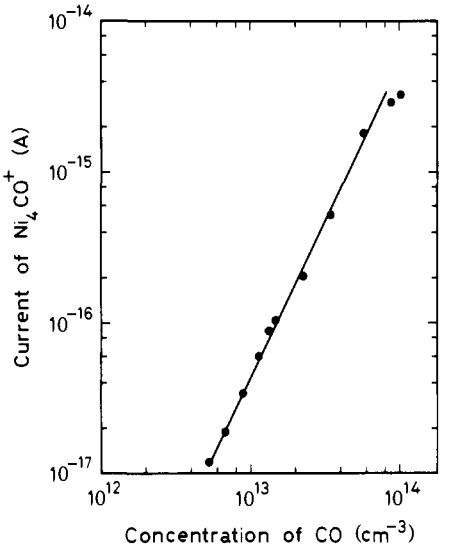

Figure 5. Log-log plot of the Ni_4CO^+ intensity vs. CO concentration exhibiting a quadratic dependence.

The pressure dependence of the compound buildup is a valuable observable for the kinetics. The intensity of the compound Ni_nCO^+ as a function of the CO concentration was systematically investigated. Figure 5 gives a typical result as obtained for Ni_4^+. A simple steady-state approximation for this result exhibits a quadratic dependence of the product intensity on the CO concentration. The reaction, therefore, is a sequential three body collision. The same result was observed for various cluster sizes except for Ni_3^+, which will be the subject of future investigations.

IV. Discussion

The organometallic chemistry of gas-phase ions has been the subject of some preliminary investigations using Fourier transform ion cyclotron resonance spectroscopy, and reactions producing clusters containing up to four or five metal atoms have been reported.[7] We here describe the controlled syntheses of some novel homoleptic nickel carbonyls, $Ni_x(CO)_y^+$, the stoichiometry of which can be related to recently developed bonding models for organometallic cages and clusters.

It is now well-established that individual carbon monoxide ligands in multimetallic complexes rapidly interchange positions intramolecularly. Often, there is no one arrangement of ligands about the central metal core which is greatly preferred energetically over all others.[8] Indeed, it is readily apparent that individual ligands are interacting with the cluster as a whole and not just

(7) Comisarow, M. B. In *Fourier, Hadamard and Hilbert Transforms in Chemistry*; Marshall, A. B., Ed.; Plenum Press: New York, 1982; pp 139–144.
(8) (a) Cotton, F. A.; Jamerson, J. D. *J. Am. Chem. Soc.* **1976**, *98*, 1273. (b) Benfield, R. E.; Johnson, B. F. G. *J. Chem. Soc., Dalton Trans.* **1980**, 1743.

with individual metal atoms. The close analogies between this situation and the bonding of the so-called "electron-deficient" boranes, B_nH_m, have been recognized by Wade and by Mingos in a series of seminal papers,[9] and there now exist simple electron-counting rules which enable us to correlate molecular geometries of metal cluster complexes with the total number of valence electrons.[10] These ideas have also been extended to account for some aspects of the reactivity of organometallic clusters.[11] Of particular relevance to the results we have obtained is the work of Lauher[12] who not only calculated the most favorable molecular geometry for any given transition metal cluster but also predicted the bonding capabilities of such clusters. The original calculations were based on clusters of rhodium atoms, but the results are readily transferable to most of the other transition metals. Since that time, many of Lauher's predictions have been experimentally verified.[13]

Typically, a tetrahedral metal cluster will be maximally stabilized when the total number of cluster valence electrons (CVE's) is 60. This total is made up of the metal valence electrons augmented by those supplied by the ligands (two from each carbon monoxide). Thus, the tetrahedral molecules $M_4(CO)_{12}$, M = Co, Rh, Ir, have been structurally characterized by X-ray crystal-

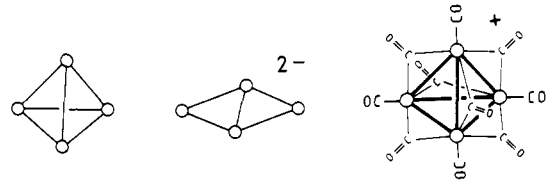

lography.[14] In contrast, the addition of two more electrons produces a less compact (more open) geometry, viz, the butterfly structure of $Re_4(CO)_{16}^{2-}$ which has 62 CVE's.[15] Hence, the $Ni_4(CO)_{10}^{+}$ ion, produced by the reaction of excess CO with Ni_4^{+}, will possess a tetrahedral arrangement of metal atoms. We note that the final peak, $Ni_4(CO)_{10}^{+}$, is much less intense than the $(P-CO)^{+}$ peak, but this is a very common occurrence in the mass spectra of metal carbonyl clusters.[16]

In the case of $Ni_4(CO)_{10}$, it is possible to draw a structure with four terminal and six bridging carbonyl ligands which prossesses full T_d symmetry and formally assigns to each nickel atom an 18-electron configuration. However, such a structure is just one of several which will lie on a potential energy surface and is not necessarily the predominant isomer. Thus, in its ground state, $Ir_4(CO)_{12}$ has T_d symmetry with 12 terminally bonded carbonyls whilst $Co_4(CO)_{12}$ and $Rh_4(CO)_{12}$ have C_{3v} structures with three of the CO's bridging the edges of one face and the remaining nine CO's all terminal.[17] Normally, for clusters of higher nuclearity, it will not be possible to draw a Lewis diagram appropriate for a localized bonding model, and these are best described by using the delocalized molecular orbital schemes mentioned previously.[9,10,12]

Clusters containing five metal atoms will have 72 CVE's if they adopt the trigonal bipyramidal geometry known for $Os_5(CO)_{16}$[18] but would require 74 CVE's for the more open square-based pyramidal structure.[19] The highest molecular weight cluster

obtained from the reaction of Ni_5^{+} and carbon monoxide corresponds to $Ni_5(CO)_{12}^{+}$. The neutral molecule $Ni_5(CO)_{12}$ has 74 CVE's and so fits nicely into the square-based pyramidal category. One should mention here that a carbonyl anion, $Ni_5(CO)_{12}^{2-}$, has been prepared by the careful reduction of nickel tetracarbonyl with alkali metals or by alkali metal hydroxides in methanol. This cluster has 76 CVE's and has been shown by X-ray crystallography to have a D_{3h} structure but very markedly elongated along the threefold axis.[20]

Following the same pattern, it has been shown that stable, octahedral, hexametallic clusters would have the maximum stability for an 86 CVE count. Now, the six nickel atoms provide 60 electrons which leaves the remaining 26 electrons to be supplied by 13 carbon monoxide ligands. It is gratifying that the highest molecular weight ion observed corresponds to $Ni_6(CO)_{13}^{+}$! The anion $Ni_6(CO_{12})^{2-}$, which has 86 CVE's, has a trigonal antiprismatic arrangement of nickel atoms (i.e., an octahedron slightly stretched along one threefold axis),[21] and molecular orbital arguments have been advanced to rationalize this distortion from idealized O_h symmetry.[22] Heptametallic carbonyl clusters have not been reported in great abundance! The viable geometries[12] are the monocapped octahedron or the pentagonal bipyramid (both with 98 CVE's) and the capped trigonal prism (102 CVE's). The

monocapped octahedron is known[23] for $Rh_7(CO)_{16}^{3-}$, which would correspond to $Ni_7(CO)_{14}$. The analogy to boron hydride chemistry would suggest that the pentagonal bipyramidal structure with all edges equal would require 100 CVE's (and hence $Ni_7(CO)_{15}$), but in the 7-vertex metallic clusters a significant interaction between the two apical metal atoms gives rise to a highly antibonding orbital of a_2'' symmetry.[12] This situation can be alleviated by an elongation of the bipyramid along the fivefold axis. In any event, the highest peak detected in our reaction of Ni_7^{+} with CO corresponds to $Ni_7(CO)_{15}^{+}$. Thus, although a clear distinction between the capped octahedron and the pentagonal bipyramid cannot be made, the capped trigonal prism appears to be ruled out.

For eight-atom clusters, the favored geometry is the triangular dodecahedron which is maximally stabilized with 112 CVE's. Such an electron count would be achieved by combining eight nickels (80 electrons) with 16 carbonyl ligands; indeed, all the peaks are observed for $Ni_8(CO)_x$ for $x = 0$–16. Interestingly, very little fragmentation to smaller nickel clusters is observed suggesting that Ni_8^{+} is a relatively stable species.

(9) (a) Wade, K. *Adv. Inorg. Chem. Radiochem.* **1976**, *18*, 1. (b) Mingos, D. M. P. *J. Chem. Soc., Dalton Trans.* **1974**, *133*.
(10) (a) Mingos, D. M. P. *Acc. Chem. Res.* **1984**, *17*, 311. (b) Mingos, D. M. P. *Chem. Soc. Rev.* **1986**, *15*, 31.
(11) McGlinchey, M. J.; Mlekuz, M.; Bougeard, P.; Sayer, B. G.; Marinetti, A.; Saillard, J.-Y.; Jaouen, G. *Can. J. Chem.* **1983**, *61*, 1319.
(12) Lauher, J. W. *J. Am. Chem. Soc.* **1978**, *100*, 5305.
(13) Johnson, B. F. G. In *Transition Metal Clusters*; Johnson, B. F. G., Ed.; Wiley-Interscience: New York, 1980.
(14) Wei, C. H. *Inorg. Chem.* **1969**, *8*, 2384.
(15) Churchill, M. R.; Bau, R. *Inorg. Chem.* **1968**, *7*, 2606.
(16) Bruce, M. I. *Adv. Organomet. Chem.* **1967**, *6*, 273.
(17) Johnson, B. F. G.; Benfield, R. E. *J. Chem. Soc., Dalton Trans.* **1978**, 1544.
(18) Eady, C. R.; Johnson, B. F. G.; Lewis, J.; Reichert, B. E.; Sheldrick, G. M. *J. Chem. Soc., Chem. Commun.* **1976**, 271.
(19) Halet, J.-F.; Saillard, J.-Y.; Lissillour, R.; McGlinchey, M. J.; Jaouen, G. *Organometallics* **1986**, *5*, 139.
(20) Longoni, G.; Chini, P.; Cavalieri, A. *Inorg. Chem.* **1976**, *15*, 302.
(21) Calabrese, J. C.; Dahl, L. F.; Cavalieri, A.; Chini, P.; Longoni, G.; Martinengo, S. *J. Am. Chem. Soc.* **1974**, *96*, 2616.
(22) Evans, J. *J. Chem. Soc., Dalton Trans.* **1980**, 1005.
(23) Albano, V. G.; Belton, P. L.; Ciani, G. F. *Chem. Commun.* **1969**, 1024.

Table II. Predicted and Observed CO Bonding Capabilities of Ni_n^+ Clusters[b]

cluster	Ni_2^+	Ni_3^+	Ni_4^+	Ni_5^+	Ni_6^+	Ni_7^+	Ni_8^+	Ni_9^+	Ni_{10}^+	Ni_{11}^+	Ni_{12}^+	Ni_{13}^+
max quant of predctd CO ligands	7	9	10	11	13	15	17	19	21	23	25	20
max quant of obsd CO ligands	9	8	10	12	13	15	16	17	18	19	20	20[a]

[a] Very small peak appearing for 21 and 22. [b] See text.

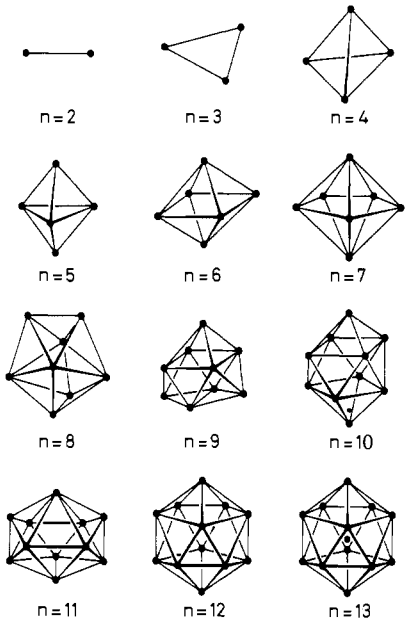

Figure 6. Shapes of polyhedral clusters Ni_n^+ where n ranges from 2 through 13.

The predicted nine-atom nickel carbonyl cluster would be $Ni_9(CO)_{19}$ with 128 CVE's and a tricapped trigonal prismatic structure. Despite the relatively low abundance of Ni_9^+ clusters, one can readily detect the ions $Ni_9(CO)_x^+$, where $x = 0$–17. Of course, as one goes toward larger clusters, the metal cluster/boron hydride analogy begins to break down, and the metal complexes are perhaps then better described as metal crystallites with a peripheral coating of ligands.[24] Thus, for clusters containing 10–13 metal atoms one cannot necessarily expect to see the electron counts corresponding to the borane–metal cluster analogy which would predict $Ni_{10}(CO)_{21}$ (142 e^-), $Ni_{11}(CO)_{23}$ (156 e^-), and $Ni_{12}(CO)_{25}$ (170 e^-). In fact, the highest molecular weight ions correspond to $Ni_{10}(CO)_{18}^+$, $Ni_{11}(CO)_{19}^+$, and $Ni_{12}(CO)_{22}^+$. These findings are in line with data on other large systems which have been crystallographically characterized.[13] A particularly interesting result is obtained for the 13-nickel system which gives very weak peaks for $Ni_{13}(CO)_{21}^+$ and $Ni_{13}(CO)_{22}^+$ but a strong peak for $Ni_{13}(CO)_{20}^+$. This latter cluster, or rather its neutral analogue $Ni_{13}(CO)_{20}$, has 170 e^- which is the exact electron count required for a nickel-centered 12-vertex polyhedron.[10b] This situation has been encountered previously in, for example, $|Rh_{13}(CO)_{24}H_3|^{2-}$ which has an encapsulated rhodium atom.

We have briefly commented on the existence in these systems of a series of clusters $Ni_nC(CO)_l^+$, and we note that in the majority of cases (see Table I) the highest molecular weight ion has two less carbonyls than does the $Ni_n(CO)_k^+$ cluster with the same number of nickel atoms. Typically, one observes $Ni_6(CO)_{13}^+$, $Ni_6C(CO)_{11}^+$ and $Ni_8(CO)_{16}^+$, $Ni_8C(CO)_{14}^+$. In these cases, it is apparent that the four skeletal electrons previously provided by two carbonyl ligands now come from a single encapsulated carbon atom in the middle of the metal cage. This phenomenon is well-documented in more conventionally synthesized molecules such as $Ru_6(CO)_{18}^{2-}$ and $Ru_6C(CO)_{17}$ which have identical skeletal electron counts.

We note also that, for the higher molecular weight clusters, the molecules $Ni_{n-1}(CO)_m^+$ which arise via fragmentation of their precursors $Ni_n(CO)_k^+$ exhibit peaks such that $m > k$. It may be that the fragmentation processes occur after carbonyl buildup is well under way so that loss of a nickel vertex leaves a relatively rigid cluster which cannot quickly collapse to the most compact (i.e., closo) geometry. One might speculate that the products derived from fragmentation processes in the presence of CO lead to open clusters. Thus, these fragment ions may have accumulated a larger number of carbonyls to saturate the open face.

It would be interesting at some future time to generate negatively charged ions and study their chemistry. In particular, there exists a series of clusters $|Pt_3(CO)_6|_n^{2-}$, when $n = 2$–6. These molecules are made up of stacks of triangular units which are built up in a spiral arrangement.[25]

Turning now to the low molecular weight clusters derived from Ni_3^+, Ni_2^+, and Ni^+, we would anticipate for the trimetallic system a triangular molecule requiring 48 CVE's. This would correspond to $Ni_3(CO)_9$, and we have so far observed peaks up to $Ni_3(CO)_8^+$.

The most stable bimetallic systems should possess 34 CVE's as do, for example, $Co_2(CO)_8$ or $Re_2(CO)_{10}$. One would thus expect to see a stable $Ni_2(CO)_7$ species which could possess one

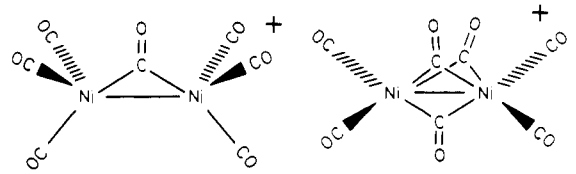

or three bridging carbonyls. If the latter situation were to be the case, the molecule would closely resemble the isoelectronic $Fe_2(CO)_9$ system in which each iron atom bonds to three terminal and three bridging ligands.[26] Interestingly, we see not only peaks up to $Ni_2(CO)_7^+$ but even weak peaks corresponding to $Ni_2(CO)_8^+$ and to $Ni_2(CO)_9^+$; this might be interpreted as extra carbon monoxides being weakly held via a van der Waals interaction. Of course, there would normally be no thermodynamic advantage to dimerization of $Ni(CO)_4$ via bridging carbonyls since that would be the only bonding, and any direct metal–metal interaction would be antibonding since only filled metal orbitals would be available. However, in the cation such an interaction would involve only three electrons rather than four so the σ^* orbital would be only half-occupied and so the overlap would lead to some degree of weak metal–metal bonding. Of course, this proviso should be applied to all the clusters synthesized herein since we are dealing with ion–molecule reactions rather than with neutrals.

Monoatomic Ni^+ reacts as expected to yield $Ni(CO)_4$, but, surprisingly, there is an intense peak corresponding to $Ni(CO)_8^+$. It would seem to be necessary to invoke van der Waals interactions perhaps by placing the four "extra" ligands on the faces of the $Ni(CO)_4^+$ tetrahedron much like a second coordination sphere in solution chemistry. At present, we prefer not to succumb to too much speculation, and we merely report the observations.

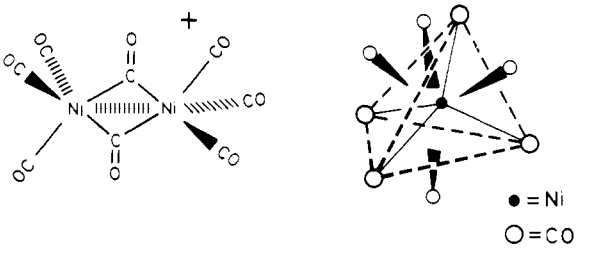

(24) Chini, P. *J. Organomet. Chem.* **1980**, *200*, 37.

(25) Calabrese, P.; Dahl, L. F.; Chini, P.; Longoni, G.; Martinengo, S. *J. Am. Chem. Soc.* **1974**, *96*, 2614.

(26) Cotton, F. A.; Troup, J. M. *J. Chem. Soc., Dalton Trans.* **1974**, 800.

V. Summary and Conclusions

It has been demonstrated that nickel cluster ions, size-selected by quadrupole mass spectrometry, react with carbon monoxide to yield complexes of the type $Ni_n(CO)_k^+$ and $Ni_nC(CO)_l^+$ where n ranges from 1 through 13 and k and l correlate extremely well with the electron-counting rules proposed by Lauher (see Figure 6 and Table II).

The data presented here were obtained primarily for the purpose of identifying the products, but, as we have already shown for Ag_n^+ clusters,[27] there is a sufficient particle flux to carry out these reactions on a synthetic scale. One can readily envisage applications to surface chemistry and to catalysis, and these will be the subject of future reports.

Acknowledgment. We thank the Institute of Experimental Physics at the Swiss Federal Institute of Technology in Lausanne and the Swiss National Science Foundation for supporting this collaborative project.

Registry No. Ni_2^+, 51404-27-4; Ni_3^+, 51404-28-5; Ni_4^+, 73145-96-7; Ni_5^+, 73145-97-8; Ni_6^+, 73145-98-9; Ni_7^+, 73145-99-0; Ni_8^+, 73146-00-6; Ni_9^+, 106543-06-0; Ni_{10}^+, 106543-05-9; Ni_{11}^+, 106567-05-9; Ni_{12}^+, 106543-07-1; Ni_{13}^+, 106543-08-2; CO, 630-08-0.

(27) Fayet, P.; Granzer, F.; Hegenbart, G.; Moisar, E.; Pischel, B.; Wöste, L. *Phys. Rev. Lett.* **1985**, *55*, 3002.

Electron Self-Exchanges in an Osmium Polypyridine Redox Polymer in the Absence of Liquid Solvents by Solid-State Voltammetry

J. C. Jernigan and Royce W. Murray*

Contribution from the Kenan Laboratories of Chemistry, University of North Carolina, Chapel Hill, North Carolina 27514. *Received August 18, 1986*

Abstract: This paper describes voltammetry in the absence of external liquid electrolytes of films of the redox polymer poly[$Os(bpy)_2(vpy)_2$]$(X)_n$ sandwiched between Pt and porous Au electrodes and bathed in acetonitrile vapor, dry N_2, 10^{-6} torr vacuum, toluene liquid, or toluene vapor. The voltammetry differs for n = 1, 2, or 2.5 and is quantitatively explained with theory based on electron diffusion in the polymer occurring by electron self-exchange reactions between polymer sites. Electron diffusion coefficients, D_e, depend strongly on the bathing medium, being the same in acetonitrile vapor and liquid for the poly[Os(III/II)] and poly[Os(II/I)] couples, but depressed for the former and elevated for the latter in films contacted only by dry N_2. The latter circumstance yields the largest electron diffusion coefficient measured thus far for a localized electronic state redox polymer, 1.7×10^{-6} cm^2/s.

Learning how to conduct quantitatively interpretable voltammetry of electrochemical reactions in the absence of liquid solvents may lead to discoveries of new chemical sensors, applications in energy storage and in macromolecular electronics, and how the kinetics and thermodynamics of electron-transfer reactions respond to solvation. Most previous solid-state electrochemical investigations[1] have focused on energy storage applications and consequently a limited range of redox couples (Li, Na), in cells fashioned from ionically conductive inorganic lattice and layer compounds. Recent applications of ionically conducting polymers[2] are, on the other hand, expanding the range of solid-state electrochemical phenomena studied, to include photoelectrochemical[3] and electrochromic[4] cells, solid-state polymer batteries,[5] an in situ UHV electron spectroscopy experiment,[6] a gas detector,[7] and electron transport in redox polymers.[8] An additional point of note is how the electron transfer chemistry of solid-state materials can yield insights into the internal dynamics of solid materials as illustrated by recent work by Hendrickson et al.[9]

In this paper, we explore how the rates of the electron self-exchange reactions between Os(III) and Os(II), and between Os(II) and Os(I), complex sites in films of the polymer[10] poly-[$Os(bpy)_2(vpy)_2$]$(X)_2$, depend upon the medium bathing the polymer film: a liquid solvent, a solvent vapor, a dry gas, or vacuum. To measure these rates, we use sandwich electrode microstructures[11] containing ca. 80–800-nm films of the poly-[$Os(bpy)_2(vpy)_2$]$(X)_2$ polymer. The steady-state currents which flow between the two metal contacts of the sandwich microstructure when their potentials are set so as to oxidize and reduce, respectively, osmium sites at the opposing metal/polymer interfaces (schematically shown in Figure 1, top) are controlled by electron self-exchanges between oxidized and reduced sites in the intervening polymer film. The rate of these self-exchanges is measured

(1) (a) Linford, R. G.; Hackwood, S. *Chem. Rev.* **1981**, *81*, 327 and references therein. (b) Raleigh, D. O. In *Electroanalytical Chemistry*; Bard, A. J., Ed.; Marcel Dekker: New York, 1973; Vol. 6.

(2) (a) Armand, M. B.; Chabagno, J. M.; Duclot, M. J. *Fast Ion Transport in Solids*; Vashishta, P., Ed.; North Holland: New York, 1979; pp 131. (b) Armand, M. B. *Solid State Ionics* **1983**, *9/10*, 745. (c) Spindler, R.; Shriver, D. F. *Macromolecules* **1986**, *19*, 347. (d) Dupon, R.; Papke, B. L.; Ratner, M. A.; Shriver, D. F. *J. Electrochem. Soc.* **1984**, *131*, 586. (e) Hardy, L. C.; Shriver, D. F. *J. Am. Chem. Soc.* **1985**, *107*, 3823. (f) Reitman, E. A.; Kaplan, M. L.; Cava, R. J. *Solid State Ionics* **1985**, *17*, 67.

(3) (a) Inganas, O.; Skotheim, T. A. *Mol. Cryst. Liq. Cryst.* **1985**, *121*, 285. (b) Inganas, O.; Skotheim, T. A.; Feldberg, S. W. *Solid State Ionics* **1986**, *18/19*, 332.

(4) Calvert, J. M.; Manuccia, T. J.; Nowak, R. J. *J. Electrochem. Soc.* **1986**, *133*, 951.

(5) (a) Schoonan, J.; Wolfert, A.; Untereker, D. F. *Solid State Ionics* **1983**, *11*, 187. (b) Matsumoto, T.; Matsunaga, K. *Bull. Chem. Soc. Jpn.* **1981**, *54*, 648. (c) Chiang, C. K. *Polymer* **1981**, *22*, 1454.

(6) (a) Skotheim, T. A.; Florit, M. I.; Melo, A.; O'Grady, W. E. *Mol. Cryst. Liq. Cryst.* **1985**, *121*, 291. (b) Skotheim, T. A.; Florit, M. I.; Melo, A.; O'Grady, W. E. *Phys. Rev. B* **1984**, *30*, 4846.

(7) (a) Pons, S.; Daschbach, J.; Fleischmann, M. 191st National Meeting of the American Chemical Society, New York, NY, 1986; ANAL 103. (b) Pons, S. ONR-NSF Workshop on Ultramicroelectrodes; Homestead, Utah, Jan 1986.

(8) Jernigan, J. C.; Chidsey, C. E. D.; Murray, R. W. *J. Am. Chem. Soc.* **1985**, *107*, 2824.

(9) (a) Lambert, Susan L.; Spiro, C. L.; Gagne, R. R.; Hendrickson, N. *Inorg. Chem.* **1982**, *21*, 68–72. (b) Mabad, B.; Cassoux, P.; Tuchagues, J. P.; Hendrickson, D. N. *Ibid.* **1986**, *25*, 1420. (c) Mabad, B.; Tuchagues, Y.; Hendrickson, D. N. *J. Am. Chem. Soc.* **1985**, *107*, 2801.

(10) (a) Calvert, J. M.; Schmehl, R. H.; Sullivan, B. P.; Facci, J. S.; Meyer, T. J.; Murray, R. W. *Inorg. Chem.* **1983**, *22*, 2151. (b) bpy is 2,2'-bipyridine and vpy is 4-vinylpyridine.

(11) (a) Pickup, P. G.; Murray, R. W. *J. Am. Chem. Soc.* **1983**, *105*, 4510. (b) Pickup, P. G.; Murray, R. W. *J. Electrochem. Soc.* **1984**, *131*, 833. (c) Pickup, P. G.; Kutner, W.; Leidner, C. R.; Murray, R. W. *J. Am. Chem. Soc.* **1984**, *106*, 1991.

0002-7863/87/1509-1738$01.50/0